Connections between plasma sheet transport, Region 2 currents, and entropy changes associated with convection, steady magnetospheric convection periods, and substorms

Larry R. Lyons,[1] Chih-Ping Wang,[1] Matina Gkioulidou,[1] and Shasha Zou[1]

Received 9 September 2008; revised 26 November 2008; accepted 22 January 2009; published 3 April 2009.

[1] Here we describe how energy-dependent magnetic drift in the presence of a pressure gradient in the direction of the drift leads to a divergence of perpendicular particle flux, and that this violates conservation of flux tube particle content. We address how, within the plasma sheet, this divergence of particle flux should be expected to lead simultaneously to the divergence of perpendicular current that drives the Region 2 (R2) current system and to significant violation of entropy conservation. The modeling results of Wang et al. (2004b) show that the above violation of entropy conservation due to magnetic drift, when taken together with magnetic field stretching, offers a resolution to the pressure crises question. On the basis of our argument that the same energy-dependent magnetic drift effect leads to the perpendicular divergence that drives the R2 field-aligned current system and the violation of entropy conservation, we suggest that the existence of the R2 current system can by itself be viewed as a signature of violation of entropy conservation. Finally, we propose that observational evidence suggests that an enhanced rate of entropy reduction and R2 currents resulting from particle divergence within the vicinity of the Harang reversal may be a critical aspect of the substorm expansion phase.

Citation: Lyons, L. R., C.-P. Wang, M. Gkioulidou, and S. Zou (2009), Connections between plasma sheet transport, Region 2 currents, and entropy changes associated with convection, steady magnetospheric convection periods, and substorms, *J. Geophys. Res.*, *114*, A00D01, doi:10.1029/2008JA013743.

1. Introduction

[2] The convection electric field in the magnetotail brings plasma in the tail plasma sheet earthward, resulting in plasma energization. Under the assumptions of ideal MHD, plasma conserves entropy as it moves adiabatically at the electric field drift velocity. *Erickson and Wolf* [1980] determined that such entropy conserving motion would lead to unrealistically high pressures in the plasma sheet and suggested that the magnetotail would not be stable to enhanced entropy-conserving convection, leading to what was referred to as the ''pressure crises.'' However, prolonged periods of enhanced convection within the plasma sheet are known to persist for up to many hours, which are referred to as convection bays [*Kokubun et al.*, 1977; *Pytte et al.*, 1978] or, more recently, as steady magnetospheric convection periods (SMCs) [*Sergeev et al.*, 1986; *Yahnin et al.*, 1994]. Their existence indicates that convection into the inner magnetosphere can exist stably for prolonged periods, implying that the energization inferred from entropy conservation by *Erickson and Wolf* [1980] does not give a full description of plasma sheet transport. Stretching of the magnetic field has been investigated as a potential solution to this problem [*Hau et al.*, 1989; *Hau*, 1991; *Erickson*, 1992], but the required amount of stretching was found to be too extreme to be able to readily allow for SMCs and to thus resolve the pressure crises.

[3] The plasma energization that occurs as plasma convects earthward into regions of increasing magnetic field is associated with magnetic drift of particles across electric equipotentials. *Tsyganenko* [1982] and *Spence and Kivelson* [1990] noted that this drift could lead to violation of the assumptions of entropy conservation and flux tube particle conservation of ideal MHD within the finite width magnetotail. This magnetic drift is energy dependent, and thus so is the particle energization. Here we first address how the energy-dependent magnetic drift leads to violation of entropy conservation, which taken together with magnetic field stretching, offers a resolution to the pressure crises question [*Wang et al.*, 2003, 2004b]. We furthermore describe how the same energy-dependent magnetic drift effect leads to a violation of conservation of flux tube particle content and therefore leads to the perpendicular divergence of perpendicular current that drives the region 2 (R2) field-aligned current system. This leads us to argue that the R2 current system and violation of entropy conservation are simultaneous aspects of the same process, i.e., divergence of particles driven by magnetic drift effect. We then use this to suggest that the existence of the R2 current system can by

[1]Department of Atmospheric and Oceanic Sciences, University of California, Los Angeles, California, USA.

Copyright 2009 by the American Geophysical Union.
0148-0227/09/2008JA013743

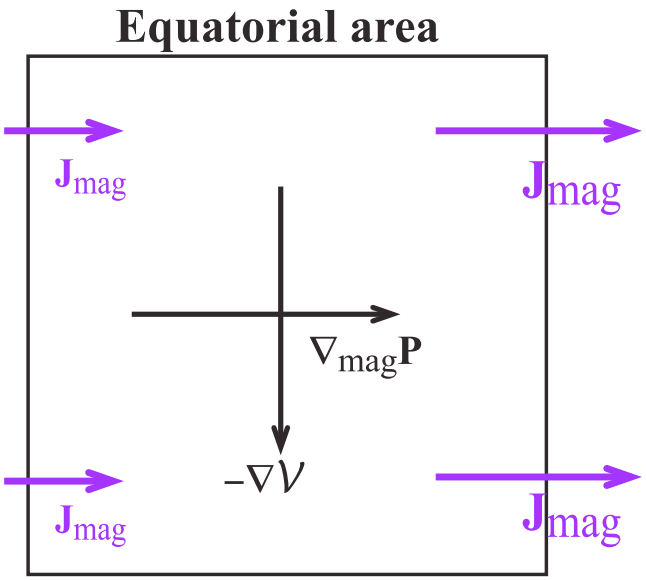

Figure 1. Illustration of how a pressure gradient in the direction of magnetic drift leads to a divergence of particle flux.

itself be viewed as a signature of violation of entropy conservation. Finally, we summarize existing evidence that the onset of the substorm expansion phase is associated with an enhancement of upward R2 currents in the region of the Harang reversal. This leads us to suggest that an enhanced rate of entropy reduction and R2 currents resulting from particle divergence within the vicinity of the Harang reversal may be a critical aspect of the substorm expansion phase.

2. Fluid Equations for Plasma Sheet Ions

[4] We consider the earthward convection of the tail plasma sheet using the equatorial ion continuity equation for flux tubes under the assumptions of isotropy and slow flow:

$$\left(\frac{\partial}{\partial t}+\mathbf{V}_E\cdot\nabla\right)(n\mathcal{V})=-\frac{\hat{\mathbf{B}}_e\cdot\nabla P\times\nabla\mathcal{V}}{qB_e}=-\frac{2}{qB_i}j_{\|,i} \quad (1)$$

Here $\mathcal{V}$ is the flux tube volume and n is the ion density, so that $n\mathcal{V}$ is the flux tube particle content. $\mathbf{V}_E$ is the electric drift velocity, q is the electronic charge, $j_{\|,i}$ is the field-aligned current density mapped to the ionosphere (positive upward from the ionosphere), and B_e and B_i are the equatorial and ionospheric field strength, respectively. The left portion of (1) is a rewritten form of the plasma sheet continuity equation obtained by *Heinemann* [1999] by integrating the single species mass conservation equation over the volume of a flux tube. The relation between $\nabla P\times\nabla\mathcal{V}$ and $j_{\|,i}$ in (1) is the well-known relation between the divergence of the plasma sheet perpendicular current and field-aligned currents for an isotropic plasma. Note that since electrons are not being included in the left portion of (1), so the application to $j_{\|,i}$ is under the assumption that the electron pressure can be neglected. Equation (1) expresses the local change in $n\mathcal{V}$ as a balance between plasma earthward convection, given by the term $\mathbf{V}_E\cdot\nabla n\mathcal{V}$, and plasma divergence driven by magnetic drift, which is given by the $\nabla P\times\nabla\mathcal{V}$ term in (1).

[5] While fundamentally important to plasma sheet dynamics, the change of flux tube particle content that results from magnetic drift is not commonly considered. This change can easily be understood physically if one considers magnetic drift within a flux tube in the presence of a pressure gradient having a component parallel to the magnetic drift velocity $\mathbf{V}_{\rm mag}$, as illustrated within the equatorial plane in Figure 1. The flux of particles per unit area from magnetic (gradient plus curvature) drift $\mathbf{J}_{\rm mag}$ can be written as $\mathbf{J}_{\rm mag}=\int f\mathbf{V}_{\rm mag}d^3\mathbf{v}$, where $\mathbf{V}_{\rm mag}$ is a function of the velocity space variable $\mathbf{v}$ and f is the phase space density. $\mathbf{V}_{\rm mag}$, and thus $\mathbf{J}_{\rm mag}$, is perpendicular to $\nabla\mathcal{V}$ [*Wolf*, 1983] as shown in the illustration. We neglect the electric drift, so that Figure 1 can be viewed as being in the frame of reference of the electric drift. Noting that $\mathbf{V}_{\rm mag}\propto K$ at a given location, where K is kinetic energy, we see that the magnitude of the particle flux $\mathbf{J}_{\rm mag}\propto P$. Thus, for a pressure gradient in the direction of the magnetic drift $\nabla_{\rm mag}P$, more particles will leave a flux tube than will enter that flux tube. There thus will be a particle flux divergence $\nabla\cdot\mathbf{J}_{\rm mag}$ within the flux tube that is proportional to the component of $\nabla_{\rm mag}P$. When integrated over a flux tube, a positive (negative) $\nabla_{\rm mag}P$ leads to loss (gain) of particles from the flux tube, which is expressed by the middle term of equation (1).

[6] Since particles are charged, the above particle flux divergence is also a divergence of perpendicular current. Such a divergence must be balanced by a field-aligned current, as given by the relation between $\nabla P\times\nabla\mathcal{V}$ and $j_{\|,i}$ in (1). This relation governs the R2 current system [e.g., *Wolf*, 1983; *Wolf et al.*, 2007]. Thus it is the divergence driven by magnetic drift that drives the R2 current systems, upward field-aligned currents occurring where the divergence is positive and downward field-aligned currents occurring where it is negative.

[7] The adiabatic assumption of ideal MHD requires that the divergence of energy flux $\mathbf{Q}$ be zero. However, in addition to carrying charge, the particles that magnetic drift in or out of a flux tube carry energy. Thus a divergence of particle flux corresponds to a divergence of energy flux as well as to a divergence of perpendicular current [*Heinemann*, 1999]. We have that $\nabla\cdot\mathbf{Q}$ is roughly proportional to $K_{\rm th}\nabla_{\rm mag}P$, where $K_{\rm th}$ is thermal energy. This implies that the divergence due to magnetic drift simultaneously drives the R2 current system and violation of entropy conservation, so that the R2 current system can be viewed as a signature of violation of entropy conservation (except, for a given $\nabla_{\rm mag}P$, in the limit of very low $K_{\rm th}$ and very high n).

[8] The effect of $\nabla\cdot\mathbf{Q}$ on entropy can be obtained from the MHD energy equation [*Siscoe*, 1983]:

$$\frac{d}{dt}\left(\frac{P}{n^{5/3}}\right)=\frac{-\nabla\cdot\mathbf{Q}+\mathbf{j}^*\cdot\mathbf{E}^*}{(3/2)n^{5/3}} \quad (2)$$

where $\mathbf{j}^*$ and $\mathbf{E}^*$ are the current density and electric field in the frame of reference moving with the plasma. The local entropy parameter $P/n^{5/3}$ in (2) can be related to the global entropy parameter per unit magnetic flux $P\mathcal{V}^{5/3}$ that is often

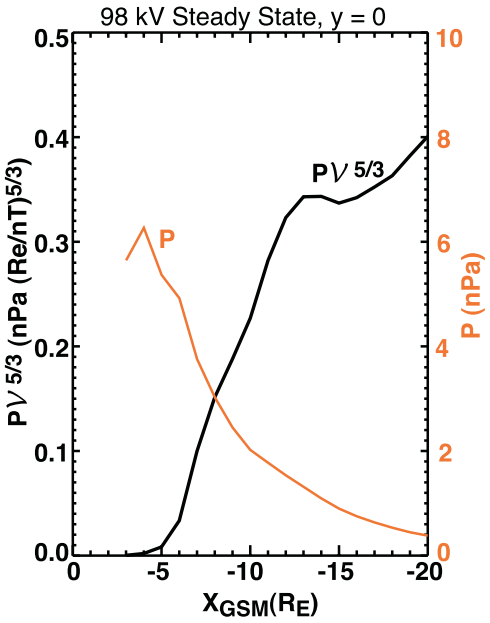

Figure 2. Equatorial proton pressure and $PV^{5/3}$ along midnight MLT meridian from the model of *Wang et al.* [2004b].

used in the study of plasma sheet particle transport [e.g., *Wolf et al.*, 2006, 2007] by

$$\frac{d}{dt}\left(PV^{5/3}\right) = (nV)^{5/3}\frac{d}{dt}\left(\frac{P}{n^{5/3}}\right) + \left(\frac{P}{n^{5/3}}\right)\frac{d}{dt}(nV)^{5/3} \qquad (3)$$

As discussed above, a positive $\nabla_{mag}P$ leads to $(d/dt)(nV) < 0$ and $\nabla \cdot \mathbf{Q} > 0$. Neglecting $\mathbf{j}^* \cdot \mathbf{E}^*$ in (2), we see that $\nabla \cdot \mathbf{Q} > 0$ gives $(d/dt)(P/n^{5/3}) < 0$. Thus, from (3), we see that such a pressure gradient will simultaneously give $(d/dt)(PV^{5/3}) < 0$ in addition to an upward field-aligned current. Similarly, we see that negative $\nabla_{mag}P$ leads to $(d/dt)(PV^{5/3}) > 0$ and downward field-aligned currents, thus completing the description of the equivalence between R2 currents and violation of entropy conservation.

3. Modeling With Energy-Dependent Magnetic Drift

3.1. Contribution of Entropy Reduction to Resolution of Pressure Crises

[9] The physics of energy-dependent magnetic drift is properly included in the Rice Convection model RCM [*Harel et al.*, 1981; *Toffoletto et al.*, 2003]. A simplified version of this model is the Magnetospheric Specification Model MSM [*Freeman et al.*, 1993]. While this model does not self-consistently calculated plasma sheet electric field distribution as does the RCM, this model was combined with the Tsyganenko 96 model [*Tsyganenko*, 1995; 1996] and the resulting model was modified to give approximate magnetic field self-consistency with the plasma pressures [*Wang et al.*, 2002]. Using this model, *Wang et al.* [2004b] were able to obtain a stable plasma sheet for SMC conditions.

[10] Figure 2 shows $PV^{5/3}$ and P versus equatorial radial distance along the midnight meridian after a several hours period of a steady, moderately enhanced cross-polar cap potential drop $\Delta\Phi_{PC}$ of 98 kV that lead to a steady state plasma sheet structure. The model results show that $PV^{5/3}$ decreases substantially along the midnight meridian, and this decrease results from the energy-dependent magnetic drift. While the plasma pressure increases toward the Earth within the plasma sheet, the plasma pressure at, for example, geosynchronous orbit is more than a factor of four lower than it would be if $PV^{5/3}$ were conserved along the midnight meridian.

[11] Figure 3 shows comparisons between the Geotail total pressures (ion plus magnetic pressure) within the central plasma sheet for quiet and substorm growth phase conditions from *Wang et al.* [2004a] and the simulated proton pressures in the equatorial plane from the *Wang et al.* [2004b] model. For this comparison, steady states with $\Delta\Phi_{PC}$ = 26 kV and 86 kV were chosen to represent quiet conditions and enhanced convection in the model. Since SMC conditions are rare, the substorm growth phase was chosen to represent enhanced convection conditions. In general the model reproduces well the observed pressure during quiet times, though the modeled pressures are slightly higher than most of the measurements at larger radial distance. The majority of the observed pressures during the substorm growth phase fall between the modeled pressures for $\Delta\Phi_{PC}$ = 26 and 86 kV. Since this range of $\Delta\Phi_{PC}$ is typical of those observed during the growth phase of substorms [*Weimer and Akasofu*, 1992], we expect most observations to fall within the two model pressure profiles. This can be seen to be the case. This shows that, with energy-dependent magnetic drift and the resultant fall off of $PV^{5/3}$ with decreasing distance to the Earth, realistic profiles of ion pressures are obtained.

[12] To further demonstrate the realism of the model results, and to demonstrate the magnetic field stretching is also important to resolving the pressure crises, we show magnetic field comparisons in Figure 4. The modeled lobe B_x (Figure 4, top) can be seen to increase with decreasing distance from the Earth and to substantially increase earthward of ~18 R_E with the increase in convection strength. Reasonable agreement can be seen with the Geotail measurement both in the radial variations and the change with convection strength. The modeled B_z in the central plasma sheet (Figure 4, bottom) decreases substantially inside of 11 R_E and increases slightly beyond ~13 R_E with the increased convection strength. The B_z observed by Geotail (beyond 8 R_E) agree in magnitude with the model and show evidence for the decrease with the increase in convection that is seen by the model earthward of 11 R_E. The data at and earthward of X_{GSM} = 6.6 R_E are from the geosynchronous GOES spacecraft. While all these data are from the vicinity of midnight, the points are plotted at the actual X_{GSM} location of their observation, so that all of these B_z measurements should be compared with the model results at geosynchronous orbit (6.6 R_E). This comparison shows that the magnitude and change with convection strength of the modeled central plasma sheet B_z at geosynchronous orbit agrees with those of those observed, which were obtained during the same quiet and growth phase periods as the Geotail observations. (Also, since the geosynchronous satellites are not always near the current sheet, we show their B_z data observations only when $|B_x| \leq 20$ nT.)

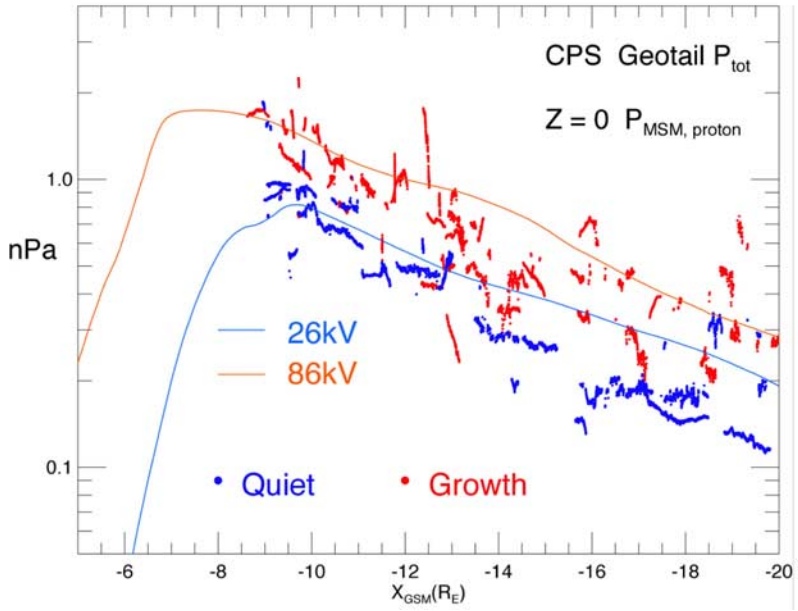

Figure 3. Comparisons between the Geotail total pressures (ion plus magnetic pressure) within the central plasma sheet (CPS) for quiet and substorm growth phase conditions from *Wang et al.* [2004a] and the simulated proton pressures in the equatorial plane from the *Wang et al.* [2004b] model for $\Delta\Phi_{PC}$ = 26 kV and 86 kV.

[13] We thus see that both the modeled pressure and force-balanced magnetic field quantitatively reproduce the observed plasma sheet under weak and enhanced convection conditions, and the difference between the two states. This is quite convincing evidence that the modeled entropy variation with radial distance is quite reasonable, and that the reduction in entropy resulting from the energy-dependent magnetic drift as the plasma sheet plasma convects earthward is indeed of fundamental importance in understanding the structure of the plasma sheet. Thus this effect, together with the stretching of the magnetic field shown in Figure 3, offers a plausible resolution to the pressure crises of *Erickson and Wolf* [1980].

3.2. Relation of Entropy Reduction to Region 2 Currents

[14] The above results were obtained with approximate self-consistency between the magnetic field and plasma. To consider the R2 currents, we turn to the RCM which includes an electric field solver that maintains current continuity simultaneously in the ionosphere and magnetosphere, thus leading to realistic modeling of both the R2 currents and the entropy reduction that simultaneously results from the energy-dependent magnetic drift. We ran the RCM using the Tsyganenko 96 magnetic field. A time-independent cross-polar cap potential drop ($\Delta\Phi_{PCP}$) of 30 kV was used for 5 h to reach a steady state quiet time plasma sheet and R2 electrodynamical system. We then increased $\Delta\Phi_{PCP}$ abruptly to 100 kV. The simulation started from a specified MLT-dependent particle distribution at the model boundary for weakly northward IMF conditions taken from a detailed statistical analysis of 11 years of Geotail observations [*Wang et al.*, 2007].

[15] Figure 5 shows, from left to right, plasma pressure, field-aligned current density, and $PV^{5/3}$. Equipotential contours are also shown in the middle plot, and the field-aligned currents are in units of ionospheric current density and are positive upward. A dashed magenta line has been sketched around the region of substantial ($\gtrsim$1 μA/m^2) upward field aligned currents. There is a channel of enhanced upward $j_{\|,i}$ running approximately along the equipotentials that are slightly premidnight and reach the inner plasma sheet region of highest pressures. Within this region, the values of $PV^{5/3}$ in the right plot slowly decrease with decreasing radial distance. Four of the equipotential contours from the middle plot are also shown in the right plot, and the decrease of $PV^{5/3}$ can be seen along the equipotential contours within the premidnight upward $j_{\|,i}$ channel. The region of enhanced upward $j_{\|,i}$ bends toward dawn at X $\sim -10\ R_E$, and can be seen to be associated with a substantial reduction in $PV^{5/3}$ in the postmidnight to dawn region. There is a downward field-aligned current region just to the dawnside of midnight beyond X $\sim -10\ R_E$, and a very small increase of $PV^{5/3}$ can be seen along the equipotential contours in this region.

[16] The above association between the R2 field-aligned currents and entropy is reflected in the modeled pressures. Substantially lower inner plasma sheet pressure can be seen along equipotentials that extend through the dawnside upward $j_{\|}$,i region than along the equipotentials that turn toward the dusk side. Of course, this results in the azimuthal pressure gradient that drives the upward R2 currents in this region. The above association with the modeled R2 currents and changes in global entropy and pressure are quite qualitative. A more quantitative comparison would require a self-consistent magnetic field model, consideration of particle losses from charge exchange and precipitation (included in the RCM and important within the innermost portions of the plasma sheet) and evaluation of entropy changes along bulk plasma drift trajectories. However, the associations discussed here qualitatively illustrate the equiv-

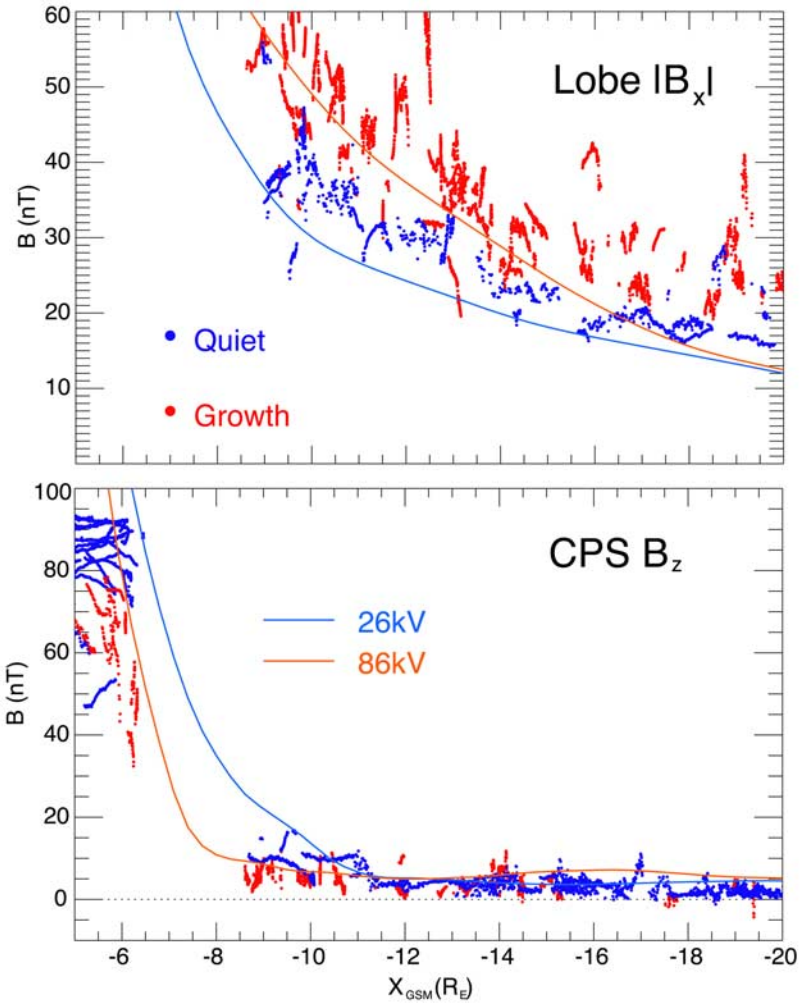

Figure 4. Comparisons of the (bottom) B_z in the equatorial plane and (top) B_x in the lobes from the *Wang et al.* [2004b] model and the Geotail CPS B_z and lobe B_x from *Wang et al.* [2004a].

alence between the R2 currents and the entropy and pressure structure of the plasma sheet.

4. Relation to Substorm Onset

[17] The auroral brightening at substorm onset is known to occur within the region of most intense proton precipitation [*Samson et al.*, 1992], typically occurring somewhat poleward of the peak of this precipitation [*Deehr and Lummerzheim*, 2001]. This corresponds to the region of the Harang electric field reversal, where R2 currents are associated with equipotentials in the vicinity of midnight that, with decreasing distance toward the Earth, first bend toward the dawnward direction and then bend duskward [*Erickson et al.*, 1991]. Substorm onset has been often observed to be associated with the Harang reversal [*Burch et al.*, 1976; *Nielsen and Greenwald*, 1978; *Baumjohann et al.*, 1981; *Nielson*, 1991; *Bristow et al.*, 2001; *Hughes and Bristow*, 2003; *Gjerloev et al.*, 2003; *Bristow and Jensen*, 2007; *Zou et al.*, 2009].

[18] The above observations place substorm auroral brightening at X ~ -8 to -10 R_E and within the inner plasma sheet region of the traditional R2 current system. This suggests that physics of violation of entropy conservation and R2 currents may play an important role in substorm onset. Furthermore, the auroral brightening at onset is associated with an enhancement of upward field-aligned currents. This suggests that there is an enhancement of entropy reduction along onset magnetic field lines in association with onset. Consistent with these inferences, the substorm expansion phase has been observed to be associated with a reduction in $PV^{5/3}$ within the inner plasma sheet [*Lyons et al.*, 2003b; *Wolf et al.*, 2006]. Furthermore, radar observations of ionospheric flows have revealed that substantial evolution of the electric fields associated with the Harang reversal occurs in association with substorms [*Bristow and Jensen*, 2007; *Zou et al.*, 2009], consistent with the dynamics of the R2 current system, and thus entropy changes, playing a significant role.

[19] If, as the above observations suggest, a reduction in global entropy is indeed a fundamental aspect of expansion phase physics, it would be important to understand how such a reduction occurs. At this time, we can only offer some speculation on this. Looking at the right plot of Figure 5, we can see the rapid earthward motion of flux tubes associated with the substorm dipolarization would bring higher-entropy

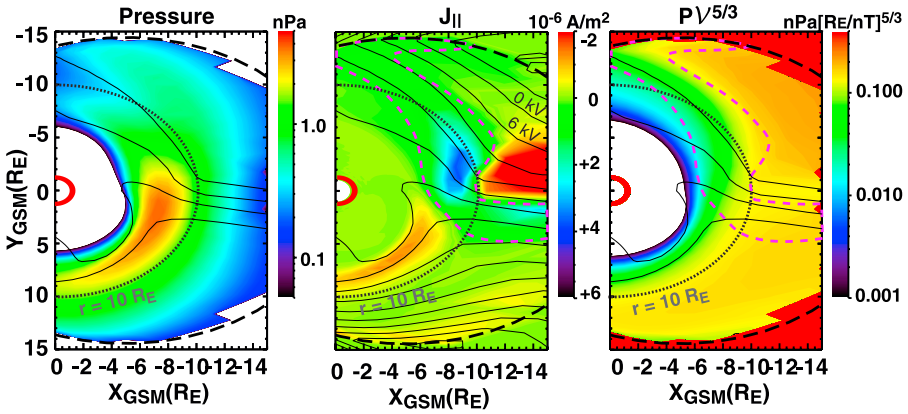

Figure 5. Plasma pressure, field-aligned current density, and $PV^{5/3}$ obtained from the RCM. $\Delta\Phi_{PCP}$ = 30 kV was used for 5 h to reach a steady state and then increased to 100 kV at T = 0. The Tsyganenko 96 magnetic field model was used, with IMF B_z decreased from 0 to −7 nT at T = 0. The boundary condition corresponds to $N_{SW} < 6.5$ nT, $V_{SW} > 400$ km/s, and 0 < IMF B_z < 1.5 nT. Results are shown at time 50 min after the enhancement. Results are shown in the equatorial plane. Pressures include both ions and electrons. In the middle plot, field-aligned currents are in units of ionospheric current density and are positive upward, and equipotential contours are separated by 6 kV. Four of these equipotentials are also shown in the left and right plots. The dashed magenta line approximately identifies the region of upward field-aligned currents and thus also of $\nabla \cdot \mathbf{Q} > 0$. The heavy dashed black line is the model outer boundary, and the dotted dashed line identifies 10 R_E equatorial radial distance.

flux tubes into the onset region. Only if something reduces the entropy of the dipolarizing flux tubes could the observed entropy reduction be explained. Reconnection that reduces the length of field lines could do this. However, on the average, substorm reconnection occurs at X ∼ −25 R_E [*Nagai et al.*, 1998; *Machida et al.*, 1999], and the initiation of entropy reduction appears to occur at the time of initial auroral brightening. This implies that entropy reduction occurs prior to substantial earthward displacement of plasma associated with dipolarization. Furthermore, entropy reduction via reconnection would first occur near X ∼ −25 R_E and then propagate toward this earthward, whereas auroral brightening occurs first in the near Earth plasma sheet and then moves to higher-latitude field lines.

[20] An alternative possibility is magnetic drift of ions from the dawnside, where the right plot of Figure 5 shows $PV^{5/3}$ is lower in response to enhanced convection than in the premidnight onset region. Duskward magnetic drift of plasma from the dawnside could be important for substorms that are associated with a reduction in the strength of convection after a growth phase period of enhanced convection, as had been inferred to be the case for many substorms [*Lyons et al.*, 2003a]. However, whether or not this could be important for entropy reduction associated with onset depends on the relative effects of the duskward magnetic drift and the earthward motion of higher-entropy plasma from larger radial distances that is associated with magnetic field dipolarization. Furthermore, this balance will be strongly affected by the energy dependence of magnetic drift and the temporal magnetic field evolution.

5. Conclusions

[21] Here we have described how energy-dependent magnetic drift in the presence of a pressure gradient in the direction of the drift leads to a divergence of perpendicular particle flux, and that this leads to violation of conservation of flux tube particle content. We described how, within the plasma sheet, this divergence of particle flux should be expected to lead simultaneously to the divergence of perpendicular current that drives the R2 current system and to significant violation of entropy conservation. On the basis of our argument that the same energy-dependent magnetic drift effect leads to the R2 field-aligned current system and to violation of entropy conservation, we suggested that the existence of the R2 current system can by itself be viewed as a signature of violation of entropy conservation. We qualitatively demonstrated this equivalence using results from the RCM under enhanced convection. Furthermore, we indicated how the modeling results of *Wang et al.* [2004b] show that the violation of entropy conservation due to magnetic drift, when taken together with magnetic field stretching, offers a resolution to the pressure crises of *Ericson et al.*, 2002].

[22] Finally, we used observational evidence, to propose that an enhanced rate of entropy reduction and of perpendicular current divergence within the inner plasma sheet, resulting from particle flux divergence within the vicinity of the Harang reversal, may be a critical aspect of the substorm expansion phase. On the basis of this proposal, we suggested that the physics of violation of entropy conservation and R2 currents may play an important role in understanding the onset of the substorm expansion phase.

[23] **Acknowledgments.** This research was supported at UCLA by National Science Foundation grants ATM-0646233 and ARC-0611717 and NASA grant NNX07AF66. We wish to thank N. A. Tsyganenko for his assistance in making modifications to the Tsyganenko 96 magnetic field model. We thank Richard Wolf at Rice University, who has generously provided us the RCM code, and Robert Spiro at Rice for helping us get the RCM running at UCLA. We also thank R. A. Wolf and F. R. Toffoletto for valuable discussion.

[24] Amitava Bhattacharjee thanks Michelle Thomsen and Jesper Gjerloev for their assistance in evaluating this paper.

References

Baumjohann, W., R. J. Pelunen, H. J. Opgenoorth, and E. Nielsen (1981), Joint two-dimensional observations of ground magnetic and ionospheric electric fields associated with auroral zone currents: Current systems associated with local auroral break-ups, *Planet. Space Sci.*, *29*, 431, doi:10.1016/0032-0633(81)90087-8.

Bristow, W. A., and P. Jensen (2007), A superposed epoch study of SuperDARN convection observations during substorms, *J. Geophys. Res.*, *112*, A06232, doi:10.1029/2006JA012049.

Bristow, W. A., A. Otto, and D. Lummerzheim (2001), Substorm convection patterns observed by the Super Dual Auroral Radar Network, *J. Geophys. Res.*, *106*, 24,593, doi:10.1029/2001JA000117.

Burch, J. L., S. A. Fields, and R. A. Heelis (1976), Substorm effects observed in the auroral plasma, in *Physics of Solar Planetary Environments*, edited by D. J. Williams, p. 740, AGU, Washington, D. C.

Deehr, C., and D. Lummerzheim (2001), Ground-based optical observations of hydrogen emission in the auroral substorm, *J. Geophys. Res.*, *106*, 33, doi:10.1029/2000JA002010.

Erickson, G. M. (1992), A quasi-static magnetospheric convection model in two dimensions, *J. Geophys. Res.*, *97*, 6505–6522, doi:10.1029/91JA03141.

Erickson, G. M., and R. A. Wolf (1980), Is steady convection possible in the Earth's magnetotail?, *Geophys. Res. Lett.*, *7*, 897–900, doi:10.1029/GL007i011p00897.

Erickson, G. M., R. W. Spiro, and R. A. Wolf (1991), The physics of the Harang discontinuity, *J. Geophys. Res.*, *96*, 1633, doi:10.1029/90JA02344.

Freeman, J. W., R. A. Wolf, R. W. Spiro, B. Hausman, B. Bales, R. Hilmer, A. Nagai, and R. Lambour (1993), Magnetospheric specification model development code documentation, scientific description, and software documentation, contract F19628-90-K-0012, Rice Univ. for Air Force Geophys. Lab., Hanscom Air Force Base, Mass., July.

Gjerloev, J. W., R. A. Hoffman, E. Tanskanen, M. Friel, L. A. Frank, and J. B. Sigwarth (2003), Auroral electrojet configuration during substorm growth phase, *Geophys. Res. Lett.*, *30*(18), 1927, doi:10.1029/2003GL017851.

Harel, M., R. A. Wolf, P. H. Reiff, and R. W. Spiro (1981), Quantitative simulation of a magnetospheric substorm: 1. Model logic and overview, *J. Geophys. Res.*, *86*, 2217–2241.

Hau, L.-N. (1991), Effects of steady state adiabatic convection on the configuration of the near-Earth plasma sheet: 2, *J. Geophys. Res.*, *96*, 5591, doi:10.1029/90JA02619.

Hau, L.-N., R. A. Wolf, G.-H. Voigt, and C. C. Wu (1989), Steady state magnetic field configurations for the Earth's magnetotail, *J. Geophys. Res.*, *94*, 1303–1316.

Heinemann, M. (1999), Role of collisionless heat flux in magnetospheric convection, *J. Geophys. Res.*, *104*, 28,397, doi:10.1029/1999JA900401.

Hughes, J. M., and W. A. Bristow (2003), SuperDARN observations of the Harang discontinuity during steady magnetospheric convection, *J. Geophys. Res.*, *108*(A5), 1185, doi:10.1029/2002JA009681.

Kokubun, S., R. L. McPherron, and C. T. Russell (1977), Triggering of substorms by solar wind discontinuities, *J. Geophys. Res.*, *82*, 74, doi:10.1029/JA082i001p00074.

Lyons, L. R., S. Liu, J. M. Ruohoniemi, S. I. Solovyev, and J. C. Samson (2003a), Observations of dayside convection reduction leading to substorm onset, *J. Geophys. Res.*, *108*(A3), 1119, doi:10.1029/2002JA009670.

Lyons, L. R., C.-P. Wang, T. Nagai, T. Mukai, Y. Saito, and J. C. Samson (2003b), Substorm inner plasma sheet particle reduction, *J. Geophys. Res.*, *108*(A12), 1426, doi:10.1029/2003JA010177.

Machida, S., Y. Miyashita, A. Ieda, A. Nishida, T. Mukai, Y. Saito, and S. Kokubun (1999), GEOTAIL observations of flow velocity and north-south magnetic field variations in the near and mid-distant tail associated with substorm onsets, *Geophys. Res. Lett.*, *26*, 635, doi:10.1029/1999GL900030.

Nagai, T., M. Fujimoto, Y. Saito, S. Machida, T. Terasawa, R. Nakamura, T. Yamamoto, T. Mukai, A. Nishida, and S. Kokubun (1998), Structure and dynamics of magnetic reconnection for substorm onsets with GEOTAIL observations, *J. Geophys. Res.*, *103*, 4419, doi:10.1029/97JA02190.

Nielson, E. (1991), Ionosphere-magnetosphere mapping of dynamic auroral structures during substorms, in *Auroral Physics*, edited by C.-I. Meng and M. J. Rycroft, p. 409, Cambridge Univ. Press, Cambridge, U. K.

Nielsen, E., and R. A. Greenwald (1978), Variations in ionospheric currents and electric fields in association with absorption spikes during the substorm expansion phase, *J. Geophys. Res.*, *83*, 5645–5654.

Pytte, T., R. L. McPherron, E. W. Hones Jr., and H. I. West Jr. (1978), Multiple-satellite studies of magnetospheric substorms: Distinction between polar magnetic substorms and convection-driven magnetic bays, *J. Geophys. Res.*, *83*, 663, doi:10.1029/JA083iA02p00663.

Samson, J. C., L. R. Lyons, B. Xu, F. Creutzberg, and P. Newell (1992), Proton aurora and substorm intensifications, *Geophys. Res. Lett.*, *19*, 2167, doi:10.1029/92GL02184.

Sergeev, V. A., A. G. Yahnin, V. O. Papitashvili, and M. V. Malkov (1986), A stationary convection study, *Prep. PGI 86-05-47*, Polar Geophys. Inst., Apatity, Russia.

Siscoe, G. L. (1983), Solar system magnetohydrodynamics, in *Solar-System Physics*, edited by R. L. Carovillano and J. M. Forbes, p. 11, D. Reidel, Dordrecht, Netherlands.

Spence, H. E., and M. G. Kivelson (1990), The variation of the plasma sheet polytropic index along the midnight meridian a finite width magnetotail, *Geophys. Res. Lett.*, *17*, 591, doi:10.1029/GL017i005p00591.

Toffoletto, F., S. Sazykin, R. Spiro, and R. Wolf (2003), Inner magnetospheric modeling with the Rice Convection Model, *Space Sci. Rev.*, *107*, 175–196, doi:10.1023/A:1025532008047.

Tsyganenko, N. A. (1982), On the convective mechanism for formation of the plasma sheet in the magnetospheric tail, *Planet. Space Sci.*, *30*, 1007, doi:10.1016/0032-0633(82)90150-7.

Tsyganenko, N. A. (1995), Modeling the Earth's magnetospheric magnetic field confined within a realistic magnetopause, *J. Geophys. Res.*, *100*, 5599–5612, doi:10.1029/94JA03193.

Tsyganenko, N. A. (1996), Effects of the solar wind conditions on the global magnetospheric configuration as deduced from data-based field models, in *Proceedings of the ICS-3 Conference on Substorms*, *Eur. Space Agency Spec. Publ., ESA-SP 389*, 181.

Wang, C.-P., L. R. Lyons, M. W. Chen, and R. A. Wolf (2002), Two-dimensional quiet time equilibrium for the inner plasma sheet protons and magnetic field, *Geophys. Res. Lett.*, *29*(24), 2186, doi:10.1029/2001GL013984.

Wang, C.-P., L. R. Lyons, M. W. Chen, R. A. Wolf, and F. R. Toffoletto (2003), Modeling the inner plasma sheet protons and magnetic field under enhanced convection, *J. Geophys. Res.*, *108*(A2), 1074, doi:10.1029/2002JA009620.

Wang, C.-P., L. R. Lyons, T. Nagai, and J. C. Samson (2004a), Midnight radial profiles of the quiet and growth-phase plasma sheet: The Geotail observations, *J. Geophys. Res.*, *109*, A12201, doi:10.1029/2004JA010590.

Wang, C.-P., L. R. Lyons, M. W. Chen, and F. R. Toffoletto (2004b), Modeling the transition of the inner plasma sheet from weak to enhanced convection, *J. Geophys. Res.*, *109*, A12202, doi:10.1029/2004JA010591.

Wang, C., L. R. Lyons, T. Nagai, J. M. Weygand, and R. W. McEntire (2007), Sources, transport, and distributions of plasma sheet ions and electrons and dependences on interplanetary parameters under northward interplanetary magnetic field, *J. Geophys. Res.*, *112*, A10224, doi:10.1029/2007JA012522.

Weimer, D. R., and S.-I. Akasofu (1992), Variations of the polar cap potential measured during magnetospheric substorms, *J. Geophys. Res.*, *97*, 3945–3951, doi:10.1029/91JA03159.

Wolf, R. A. (1983), The quasi-static (slow-flow) region of the magnetosphere, in *Solar Terrestrial Physics*, edited by R. L. Carovillano and J. M. Forbes, p. 303, D. Reidel, Norwell, Mass.

Wolf, R. A., V. Kumar, F. R. Toffoletto, G. M. Erickson, A. M. Savoie, C. X. Chen, and C. L. Lemon (2006), Estimating local plasma sheet $PV^{5/3}$ from single-spacecraft measurements, *J. Geophys. Res.*, *111*, A12218, doi:10.1029/2006JA012010.

Wolf, R. A., R. W. Spiro, S. Sazykin, and F. R. Toffoletto (2007), How the Earth's inner magnetosphere works: An evolving picture, *J. Atmos. Sol. Terr. Phys.*, *69*, 288, doi:10.1016/j.jastp.2006.07.026.

Yahnin, A., et al. (1994), Features of steady magnetospheric convection, *J. Geophys. Res.*, *99*, 4039, doi:10.1029/93JA02868.

Zou, S., L. R. Lyons, C.-P. Wang, A. Boudouridis, J. M. Ruohoniemi, P. C. Anderson, P. L. Dyson, and J. C. Devlin (2009), On the coupling between the Harang reversal evolution and substorm dynamics: A synthesis of SuperDARN, DMSP, and IMAGE observations, *J. Geophys. Res.*, *114*, A01205, doi:10.1029/2008JA013449.

M. Gkioulidou, L. R. Lyons, C.-P. Wang, and S. Zou, Department of Atmospheric and Oceanic Sciences, University of California, 405 Hilgard Avenue, 7127 Math Sciences, Los Angeles, CA 90095-1565, USA. (larry@atmos.ucla.edu)